System Identification to Estimate the Nonlinear Modes of a Gong

Daniel Piombino,
Mathew S. Allen
Department of Engineering Physics
University of Wisconsin
Madison, WI 53706
piombino@wisc.edu, msallen@engr.wisc.edu
David Ehrhardt, Tim Beberniss & Joseph Hollkamp
Air Force Research Laboratory, Dayton, OH
david.ehrhardt.1.ctr@us.af.mil, timothy.beberniss@us.af.mil & joseph.hollkamp@us.af.mil

ABSTRACT

Nonlinear Normal Modes (NNMs) have proven useful in a few recent works as a basis for comparing nonlinear models during model updating. In prior works the authors have used force appropriation to measure NNMs, but this is time consuming, generally requiring hand tuning of both the frequency in question and the strength of its harmonics. This paper explores the use of system identification, using a small set of broadband response data, to estimate a model from which the NNMs can be extracted. The Frequency Domain Restoring Force Surface (RFS) method will be used to perform identification, in which the nonlinearity of the system is assumed to be a polynomial function of the modal displacements, and a least squares problem is formed to solve for the nonlinear coefficients. Existing NNM calculation approaches can then be applied to the experimentally determined model in order to calculate the NNMs of the system. This approach is evaluated by applying it to full-field measurements from a traditional Gong, obtained using Stereo 3D Digital Image Correlation (3D-DIC). The results obtained using system identification are validated with measurements of the NNMs obtained using force appropriation and a scanning laser vibrometer.

Keywords: reduced order modeling, implicit condensation, vibration musical instrument, model updating.

1. Introduction

In extreme environments, the skin panels of high speed vehicles can experience large fluctuating pressures [1], so that geometric nonlinearity can become important, causing dramatic shifts in the resonance frequencies or even causing emergent behavior such as jump phenomena, superharmonic resonance or changes in the deformation pattern [2] and hence the stresses that the panel experiences. For constrained structures such as a pinned-pinned beam, geometric nonlinearity typically becomes important as the vibration amplitude approaches the panel thickness. Prior works [3-5], have shown that linear models are unable to provide reliable predictions in this regime, and so nonlinear models must be considered to obtain reasonable estimates of the vehicle's life. In many cases geometric nonlinearity is actually beneficial, since it may cause the resonance to de-tune itself or distribute the stress in the panel more evenly than the linear modes; hence, if reliable models of these structures could be created then it might be possible to exploit nonlinearity to create significantly lighter structures.

While modeling methods for these types of structures have advanced considerably in the past decade or two [1, 4, 6], far fewer works have explored model updating strategies or even how to comprehensively compare simulation results with measurements. This is important, as our experience with linear aerospace structures has taught us that Finite Element Models (FEMs) are almost never predictive; except for the simplest structures, some level of model tuning or model updating is always needed. In many cases significant effort is needed to update the FEM to bring it into agreement with measurements.

In [2, 7], Ehrhardt, Allen and Beberniss proposed to update finite element models for geometrically nonlinear structures by comparing their Nonlinear Normal Mode (NNM) backbone curves derived from both the FEM and measurements. The NNMs used here follow the modified Rosenberg [8] definition, and are simply periodic solutions to the undamped, nonlinear equation of motion [9, 10]. In [2, 7], the NNMs of the FEM were computed

using a reduced order model, as described in [6]. The NNMs were extracted from test using force appropriation, as proposed by Peeters et al. [11, 12], and the methodology was further developed in [13].

While previous works have shown that it is possible to measure NNMs using force appropriation, this poses a few challenges. First, a sinusoidal input must be applied, which typically precludes the use of most non-contact excitation devices. Furthermore, recent works (not yet published), have often found that multiple, synchronized shakers may be needed to adequately isolate the NNMs of more complicated structures. Second, even when force appropriation is possible, it is still quite time consuming. As an alternative, Noel et al. [14] proposed to use a two tiered approach in which a pseudo-random broadband input is first applied and a system identification algorithm is used to fit a model to the structure. The NNMs can then be derived from the identified model once the damping forces have been eliminated.

This work explores this paradigm in more detail, with several variations to what was done by Noel et al. [14]. First, whereas Noel et al. utilized a frequency domain nonlinear subspace algorithm, this work employs a far simpler method, the frequency domain Restoring Force Surface method (RFS). Second, the system treated by Noel et al. had discrete nonlinearities that could be described in terms of displacements of a few points on the structure. The structures studied here have distributed, geometric nonlinearities, and so the identification is performed in the modal domain, where the model is assumed to contain stiffness terms that are quadratic and cubic functions of the displacements of the modal displacements, which are found by applying a modal filter based on the vibration modes of the underlying linear system. To the best of the authors knowledge, the first work to employ a similar system identification approach was that of Spottswood et al. [15, 16], although they used the Nonlinear Identification through Feedback of the Output (NIFO) algorithm, which is described in the review [17].

The paper is organized as follows. Section 2 outlines the approach used. In Section 3 the proposed techniques are applied to a circular Gong, a musical instrument whose unique sound comes about due to geometric nonlinearity [18-20]. The conclusions are then presented in Section 4.

2. Theoretical Development

Geometric nonlinearity can be accurately captured by finite element models, which describe the system with a conservative equation of motion of the following form,

$$\mathbf{M}\ddot{\mathbf{x}} + \mathbf{K}\mathbf{x} + \mathbf{f}^{nl}\left(\mathbf{x}\right) = \mathbf{f}^{ex}\left(t\right) \tag{1}$$

where $\mathbf{M}$, and $\mathbf{K}$ are the $N \times N$ linear mass and stiffness matrices, $\mathbf{f}^{nl}\left(\mathbf{x}\right)$ are the nonlinear forces due to geometric nonlinearity and $\mathbf{f}^{ex}\left(t\right)$ represents the applied forces. The nonlinear normal modes of this system are the solutions $\mathbf{x}\left(t\right)$ to the equation of motion above when $\mathbf{f}^{ex}\left(t\right) = 0$, and are denoted $\mathbf{x}^{NNM}\left(t\right)$.

$$\mathbf{M}\ddot{\mathbf{x}}_{NNM} + \mathbf{K}\mathbf{x}_{NNM} + \mathbf{f}^{nl}\left(\mathbf{x}_{NNM}\right) = 0 \tag{2}$$

The NNMs of a system such as this can be computed using the method in [21], which is expensive but operates on the FEM directly, or by reducing the model and applying the algorithm by Peeters [22], a harmonic balance approach (see [23] for an excellent implementation and a through review of prior literature). See the references cited here and also [6] for further details.

The actual test hardware can be assumed to obey a similar governing equation, but realistic structures exhibit energy dissipation, which must also be considered. In the absence of additional information, this work assumes that either a modal damping or a linear viscous damping model is appropriate.

$$\mathbf{M}\ddot{\mathbf{x}} + \mathbf{C}\dot{\mathbf{x}} + \mathbf{K}\mathbf{x} + \mathbf{f}^{nl}\left(\mathbf{x}\right) = \mathbf{f}^{ex}\left(t\right) \tag{3}$$

Force appropriation methods [11, 12] seek to find a force, $\mathbf{f}^{ex}\left(t\right)$, that approximately cancels the damping forces in the structure. For example, if the applied force is a pure sinusoid at frequency ω_1 (including higher harmonics)

$\mathbf{f}^{ex}(t) = \sum_k \mathbf{a}_k \sin(k\omega_1 t)$ and the displacement, $\mathbf{x}(t)$, is a pure cosine (also including higher harmonics) $\mathbf{x}(t) = \sum_k \mathbf{b}_k \cos(k\omega_1 t)$, and if the nonlinearities are purely polynomial functions of the displacements (e.g. $x_1^2, x_1^3, x_1 x_2^2$, etc…) then because the sine and cosine functions are orthogonal, the equation of motion can be separated into the two equations below.

$$\mathbf{M}\sum_k -k^2\omega_1^2 \mathbf{b}_k \cos(k\omega_1 t) + \mathbf{K}\sum_k \mathbf{b}_k \cos(k\omega_1 t) + \mathbf{f}^{nl}\left(\sum_k \mathbf{b}_k \cos(k\omega_1 t)\right) = 0 \tag{4}$$

$$\mathbf{C}\sum_k -k\omega_1 \mathbf{a}_k \sin(k\omega_1 t) = \sum_k \mathbf{a}_k \sin(k\omega_1 t) \tag{5}$$

The top equation is simply a variant of eq. (2), the equation that is solved to obtain the NNMs of the system. Equation (5) can be used to determine the force that must be applied so that the response of the system will be equivalent to an NNM. In general, eq. (5) defines a force that must be applied at every point on a structure, which is clearly not feasible. Fortunately, various works have shown that one can obtain a very good approximation to the NNM so long as eq. (5) is satisfied in an average sense, or more specifically, if the power input over one cycle of vibration equals the power dissipated by damping [24, 25].

2.1 System Identification Methods

As mentioned earlier, the force appropriation method requires that one apply a carefully tuned sinusoidal force, which typically requires a contact exciter such as a shaker, and it can be time consuming to adjust the forcing so that Eqs (4)- (5) are satisfied. Furthermore, recent experiences have shown that for many structures it may be very difficult to adequately isolate the modes of interest using only one shaker, and applying multiple shakers complicates the method considerably. The alternative is to apply an arbitrary input and use system identification to identify a model for the system, and then to extract the NNMs from the identified model in order to understand it and to compare it with the FEM.

This work uses the frequency domain restoring force surface method, following the same procedure outlined in [26]. In summary, the method assumes that the system is describable by a modal model with nonlinear coupling terms between the modes. Specifically, if we apply the modal transformation $\mathbf{x}(t) = \mathbf{\Phi}_m \mathbf{q}(t)$ to eq. (1), where the basis vectors $\mathbf{\Phi}_m$ are the linearized modes or solutions to $\left(\mathbf{K} - \omega_r^2 \mathbf{M}\right)\boldsymbol{\varphi}_r = 0$, then one obtains the following,

$$\ddot{q}_r + \omega_r^2 q_r + \theta_r(q_1, q_2, \ldots, q_m) = \boldsymbol{\varphi}_r^{\mathrm{T}} \mathbf{f}(t) \tag{6}$$

Where the nonlinear term $\theta_r(\mathbf{q}) = \boldsymbol{\varphi}_r^{\mathrm{T}} \mathbf{f}_{NL}(\mathbf{\Phi}_m \mathbf{q})$ can be assumed to have the following polynomial form.

$$\theta_r(q_1, q_2, \ldots, q_m) = \sum_{i=1}^{m}\sum_{j=i}^{m} B_r^{ij} q_i q_j + \sum_{i=1}^{m}\sum_{j=i}^{m}\sum_{k=j}^{m} A_r^{ijk} q_i q_j q_k \tag{7}$$

A modal filter is applied based on the measured linear modes to estimate the modal displacements (from DIC data), i.e.

$$\mathbf{q}(t) = \mathbf{\Phi}_m^{\dagger} \mathbf{x}(t) \tag{8}$$

Then each of terms on the right hand side of eq. (7) can be determined from the time histories $q_j(t)$. The modal velocity and acceleration are determined by differentiating $q_j(t)$, and then all of the signals are transferred to the frequency domain to obtain a least squares problem as shown below, where the FFTs of the signals are represented with capital letters, e.g. $Q_j(\omega) = FFT\left(q_j(t)\right)$, $Q_j^v(\omega) = FFT\left(\dot{q}_j(t)\right)$, $Q_j^a(\omega) = FFT\left(\ddot{q}_j(t)\right)$, $Q^{112}(\omega) = FFT\left(q_1(t)^2 q_2(t)\right)$, etc….

$$Q_r^a(\omega)+2\zeta_r\omega_r Q_r^v(\omega)+\omega_r^2 Q_r(\omega)+A_r^{111}Q^{111}(\omega)+A_r^{112}Q^{112}(\omega)+\cdots=\boldsymbol{\varphi}_r^{\mathrm{T}}\mathbf{F}(\omega) \tag{9}$$

$$\begin{bmatrix} Q_r^v(\omega_1) & Q_r(\omega_1) & Q^{111}(\omega_1) & Q^{112}(\omega_1) & \cdots \\ Q_r^v(\omega_2) & Q_r(\omega_2) & Q^{111}(\omega_2) & Q^{112}(\omega_2) & \cdots \\ \vdots & \vdots & \vdots & \vdots & \ddots \end{bmatrix} \begin{bmatrix} 2\zeta_r\omega_r \\ \omega_r^2 \\ A_r^{111} \\ A_r^{112} \\ \vdots \end{bmatrix} = \begin{bmatrix} \boldsymbol{\varphi}_r^{\mathrm{T}}\mathbf{F}(\omega_1)-Q_r^a(\omega_1) \\ \boldsymbol{\varphi}_r^{\mathrm{T}}\mathbf{F}(\omega_2)-Q_r^a(\omega_2) \\ \vdots \end{bmatrix} \tag{10}$$

The frequencies where significant excitation can be seen are included in the least squares problem, which is solved to obtain a model for the nonlinear system. Then the damping terms can be eliminated and the modes of the model found using the NNM computation algorithm in [22].

It is important to assure that the matrix on the left in eq. (10) is well conditioned so that a unique solution can be obtained. To address this, initially models were only fit to a single mode in isolation, i.e. neglecting any modal coupling terms such as A_r^{112}, and then terms were added to the nonlinear model one at a time, and were only retained if they improved the fit to the measurements noticeably. This made it possible to minimize the number of unknowns in the curve fit while including any terms that were found to be important.

3. Experimental Application

The proposed approach was applied to the system depicted in Fig.1, which consists of a small gong suspended from a metal frame by a rope.

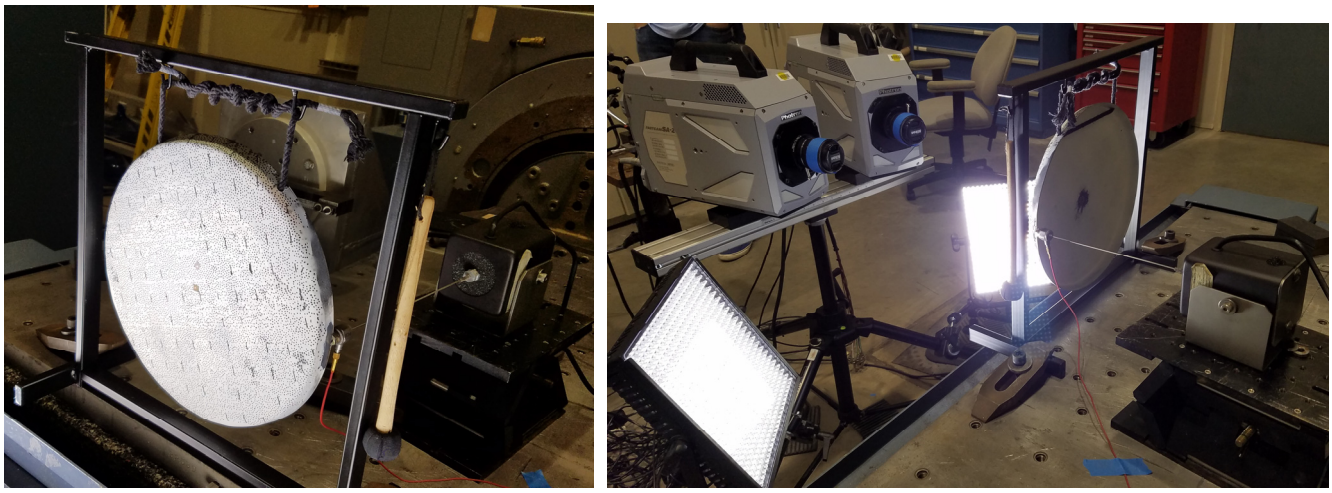

Figure 1. Photographs of setups used for DIC tests for system identification. (a) Front view of gong. (b) Photograph showing shaker setup, lighting and DIC system. Two LDVs were also used, which are part of the hardware seen behind the leftmost DIC camera.

Two Photron cameras were used to capture images of the gong at a rate of 2000 frames/second while a National Instruments PXI-Chassis recorded the response of two Polytec fiberoptic LDVs and a load cell at 5000 samples per second. The load cell was attached to the gong on the outer rim, and to a small electrodynamic shaker, which was used to excite the system.

3.1 Linear System Identification

A low amplitude pseudo-random input, band limited from 100 to 900 Hz was first applied to the system, and the response recorded for 22 seconds. The spectra of the signals were then calculated using a Hanning window with a blocksize of 4.096 seconds, which resulted in 9 averages at a 50% overlap. The H_1 estimator [27] was then used to calculate the displacement frequency response matrix of the system with respect to the measured force exerted by the shaker. The Frequency Response Functions (FRFs) obtained are shown in Fig. 2. The x- and y- direction

DIC measurements were always at least an order of magnitude smaller than those in z (out-of-plane) and they were quite noisy, so they were ignored.

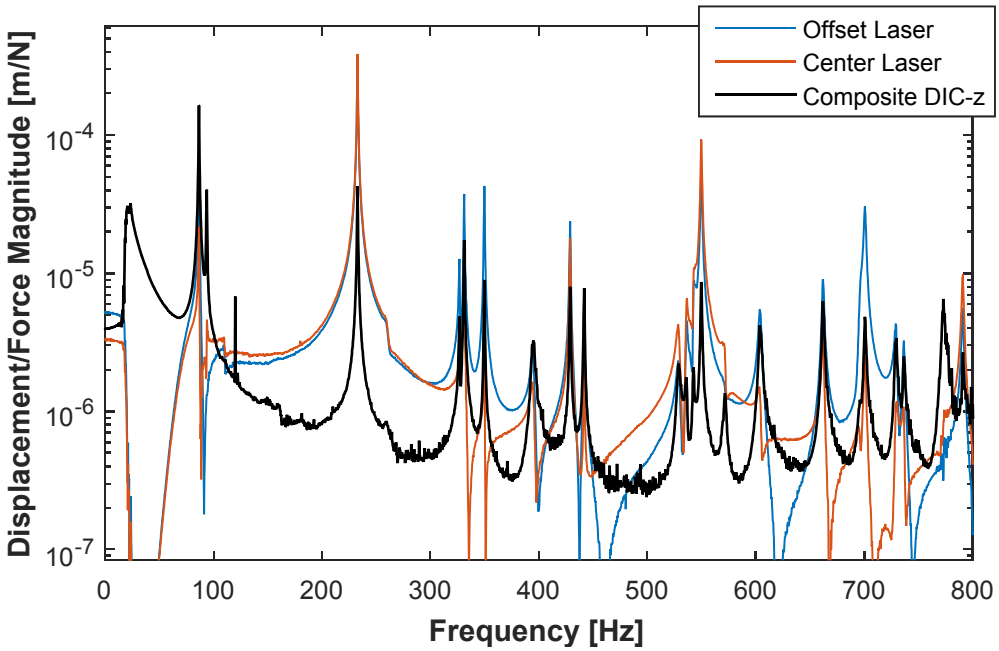

Figure 2. Low-amplitude (linear) Displacement/Force FRFs measured on the Gong using two LDVs and the DIC measurements. The DIC measurements consisted of 388 points distributed over the surface of the plate, and the composite or average of all of the out-of-plane DIC FRFs, is shown.

The Algorithm of Mode Isolation [28] was used to fit 17 modes to the DIC data and obtain their natural frequencies, damping ratios, and mode shapes. The frequencies and damping ratios of the identified modes can be found in Table 1. The corresponding mode shapes are shown in Fig. 3.

Table 1: Linear modal parameters identified from the low-amplitude DIC measurements

Mode Number	Natural Frequency [Hz]	Percent Damping
1	86.63	0.25 %
2	93.72	0.20 %
3	232.74	0.11 %
4	326.75	0.12 %
5	331.01	0.09 %
6	349.72	0.03 %
7	394.58	0.19 %
8	428.71	0.06 %
9	441.60	0.06 %
10	528.60	0.23 %
11	535.80	0.16 %
12	542.40	0.10 %
13	549.60	0.06 %
14	571.45	0.16 %
15	603.92	0.10 %
16	661.87	0.07 %
17	700.55	0.05 %
18	86.63	0.25 %
19	93.72	0.20 %

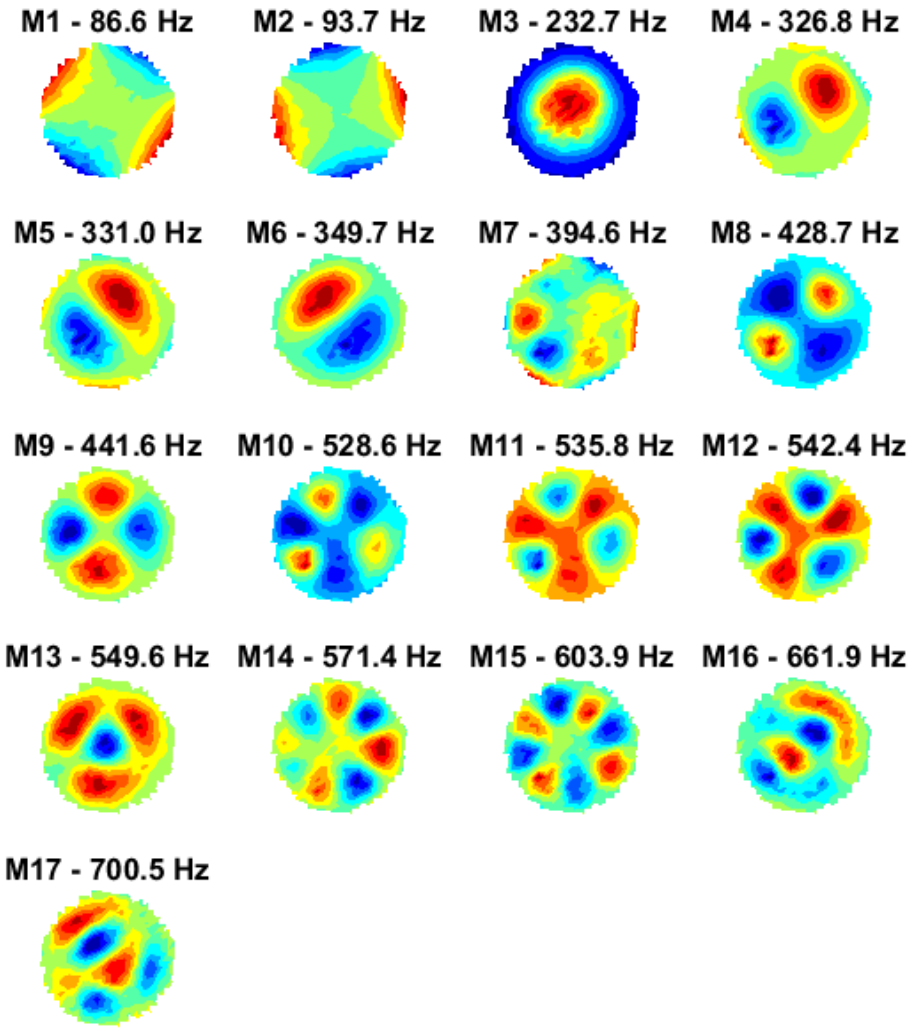

Figure 3. Mode shapes identified by AMI from the DIC measurements.

It is important that the set of modes be independent on the coordinate set if we are to obtain accurate system identification results. To evaluate this, the Modal Assurance Criterion (MAC) [29] of the mode shapes was computed and is shown in Fig. 4. This reveals two pairs of modes that are indistinguishable on the measurement set, but fortunately neither is one of the modes that is expected to exhibit the most nonlinearity. After eliminating those modes, the linear FRFs were modally filtered to test the ability of these shapes to uncouple the modes of the system. The resulting modal FRFs are shown in Fig. 5, and show that the remaining modes are capable of adequately uncoupling the system for frequencies below 700 Hz.

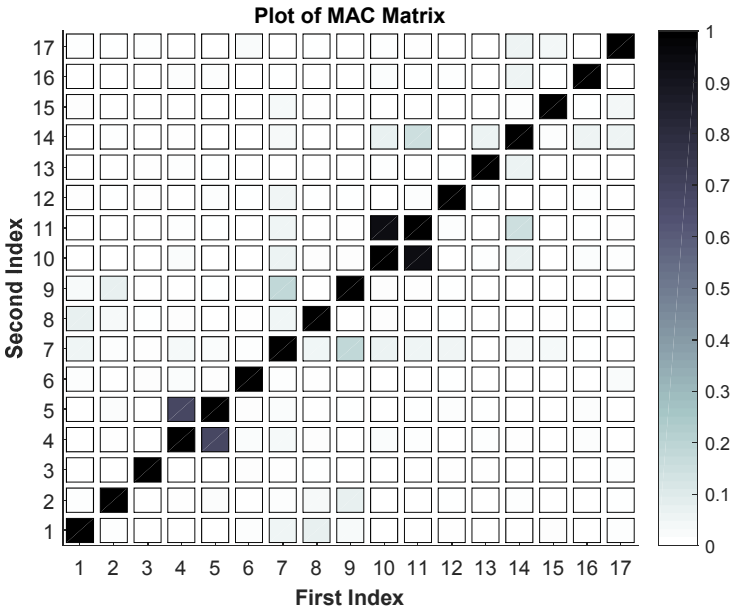

Figure 4. Auto-MAC between mode shapes identified by AMI from the DIC measurements. This reveals which modes are linearly dependent on the measurement set.

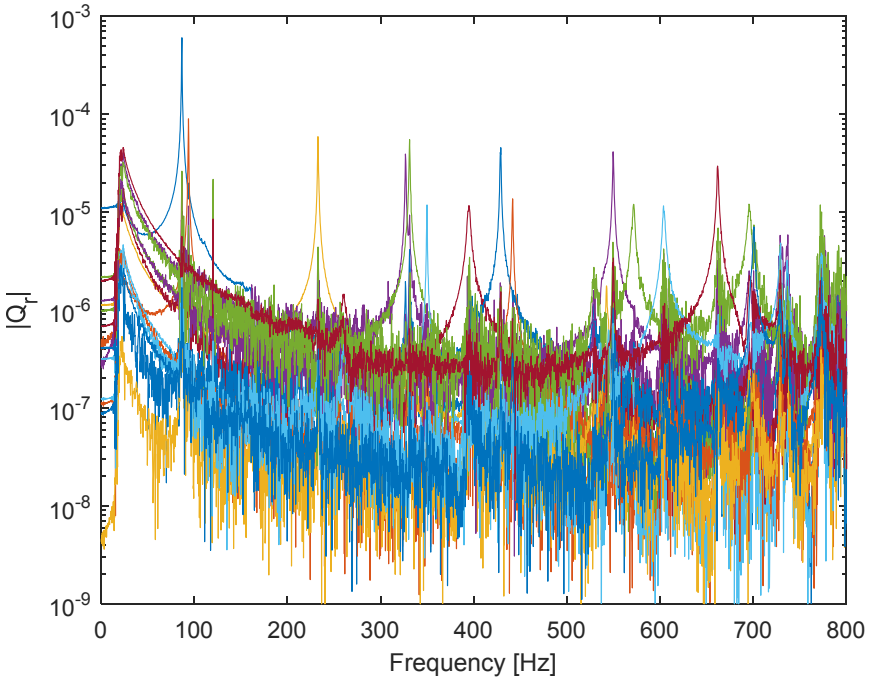

Figure 5. Linear FRFs, modally filtered to isolate each mode.

3.2 Force Appropriation

The experimental setup used to perform force appropriation was similar to that used for DIC, but employed a larger shaker and a more secure means of attaching the load cell to the gong. This testing was performed in a different lab, where the DIC system was not available, so instead Polytec PSV-400M scanning laser vibrometer was used to capture the response of the gong. The experimental setup is shown in Fig. 6. The velocity of the center of the plate was monitored using the LDV along with the force measured by the load cell, and the procedure described in [13] was used to manually adjust the frequency and amplitude of the input signal until the force and velocity were in phase, as evidenced by a Lisajous figure, indicating that the system was vibrating near

an NNM. Then the step-scanning feature in the Polytec software was used to capture the vibration of the plate over several cycles, at a grid of 121 points.

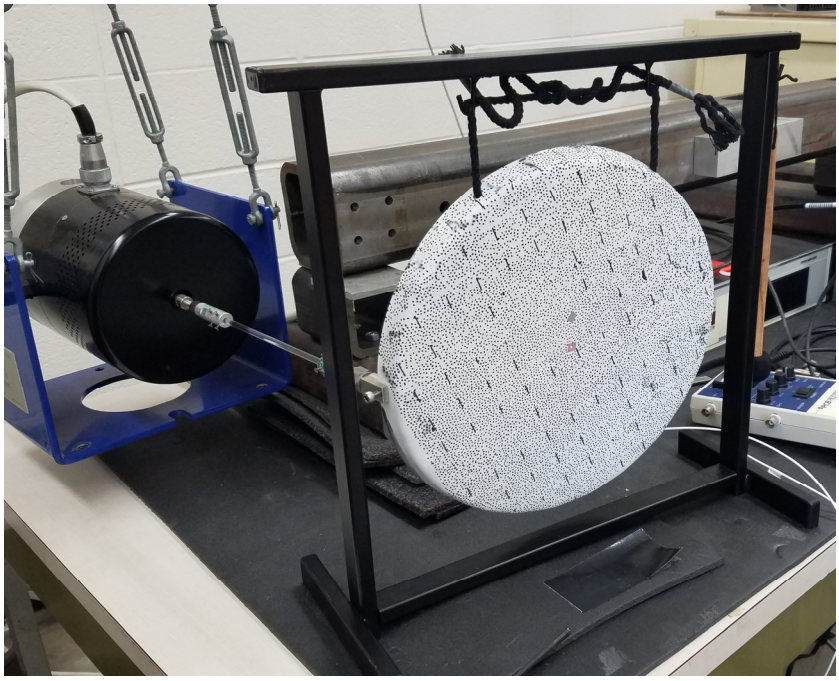

Figure 6. Photograph of test setup used to perform force appropriation to estimate the NNMs of the Gong.

The NNMs of the ~230Hz and ~550Hz modes of the system were measured in this manner. The recorded natural frequency at each excitation level was plotted against the RMS velocity of the center of the gong, and can be seen in Figures 7 and 8. The modes of a circular plate are typically labeled (d,c) according to the number of node lines parallel to a diameter and those that follow the circumference, respectively. If the outer edge of the gong is considered to be fixed, then these two modes of interest would be the (0,0) and (0,1) modes, respectively and they shall be referred to as such for the remainder of the work. The first two modes of the gong, shown in Fig. 3 would be the (2,0) modes, and so forth.

The first NNM shows only hardening behavior over the range of amplitudes tested, exhibiting about a 0.7% frequency shift. This is a small nonlinearity, but the shift in the frequency was certainly noticeable in the force appropriation process; the Lisajous figure would change visibly due to changes in the drive frequency of only 0.01 Hz. The second NNM shows both softening and hardening, with the frequency decreasing in the softening region by 0.03%, followed by a 0.1% increase in the frequency.

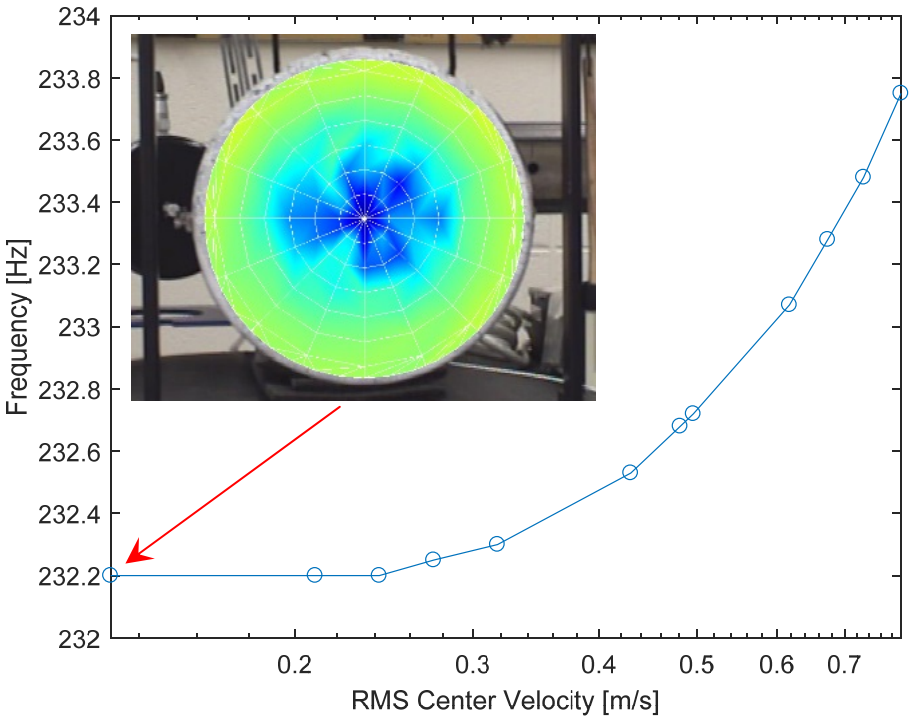

Figure 7. NNM frequency vs center point RMS velocity for the (0,0) of the gong, measured using force appropriation.

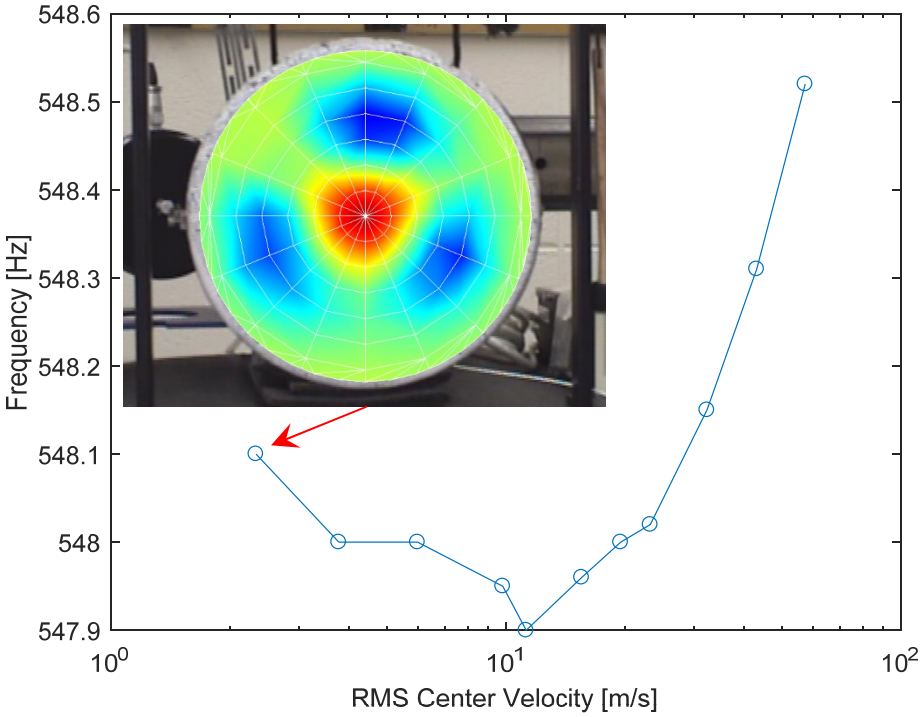

Figure 8. NNM frequency vs center point RMS velocity for the (0,1) mode of the gong, measured using force appropriation.

3.3 Nonlinear System Identification

A swept sine from 225 to 245 Hz with a 1 Hz/s sweep rate, resulting in an RMS amplitude of 13.8 N was then applied in order to nonlinearly excite the system near the (0,0) mode and data was recorded over 34 seconds, encompassing a sweep up from 225 to 245 Hz, followed immediately by a sweep down from 245 to 231 Hz. The mode shapes obtained in Section 3.1 were used to determine the modal response of the system which was converted to the frequency domain via an FFT.

Before fitting the response data to a nonlinear model, the frequency response of the (0,0) mode was compared to the response predicted by the linear FRF due to the measured forcing, which can be seen in Figure 9. Similar plots for the (0,1) mode can be seen in Figure 10. For the (0,0) mode, which is directly excited by the forcing, there is a clear over-prediction of the response by the linear model at the resonance frequency. In the measured response the system does not achieve as large of an amplitude at the linear natural frequency since the effective resonance shifts due to nonlinearity.

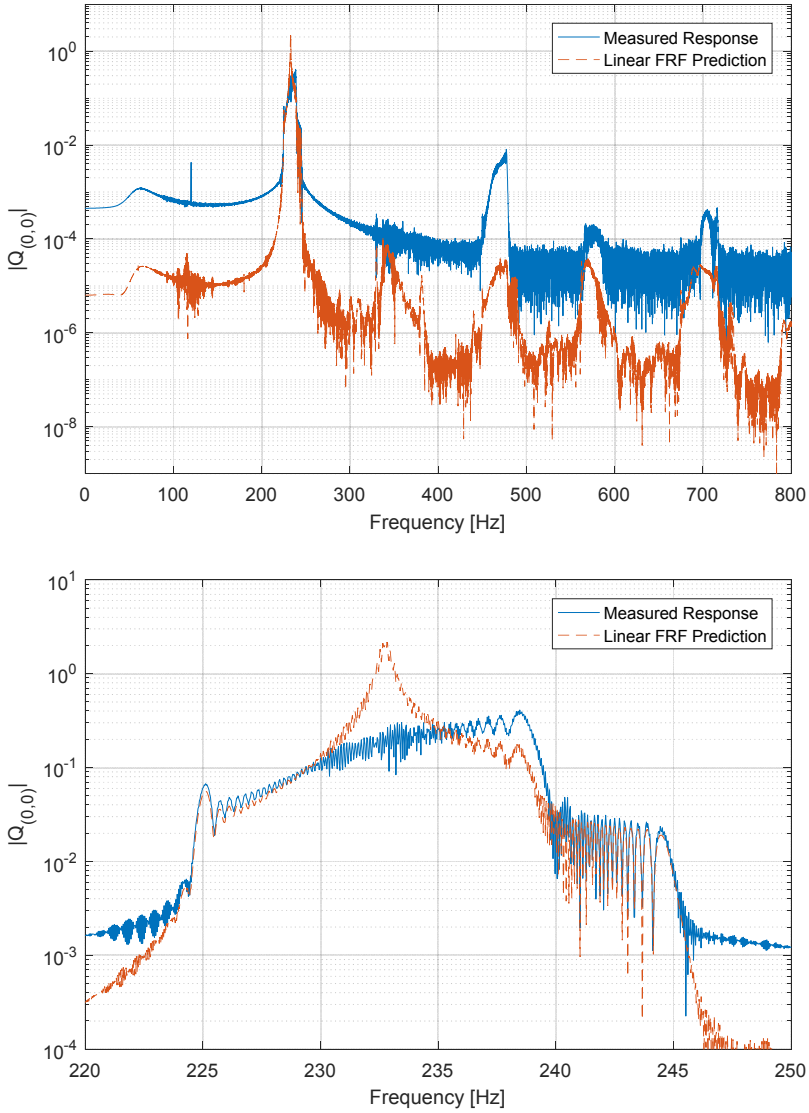

Figure 9: Measured frequency response of (0,0) mode compared to linear FRF prediction. (top) across the entire frequency range of interest, (bottom) across the excited frequency band

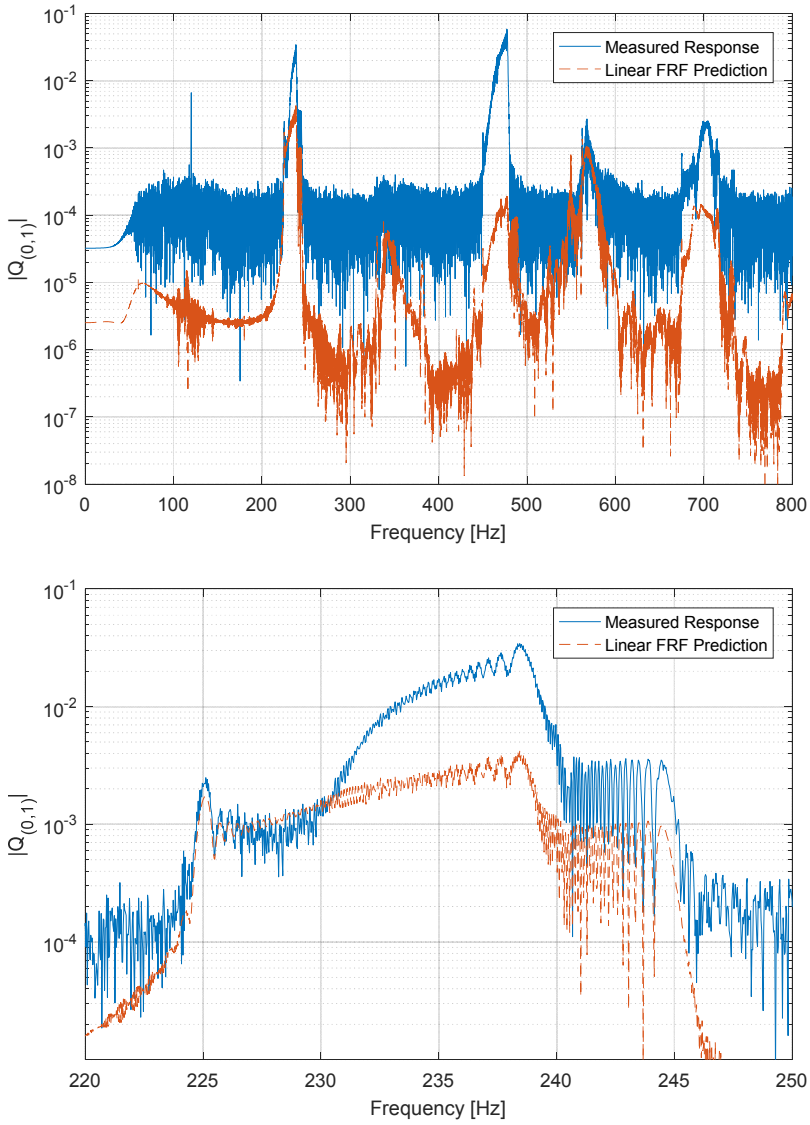

Figure 10: Measured frequency response of (0,1) mode compared to linear FRF prediction. (top) across the entire frequency range of interest, (bottom) across the excited frequency band

Although the input signal was a swept sine ranging from 225 to 245 Hz, nonlinearity in the system causes the force to be non-negligible at some other frequencies, and this causes the response predicted with the linear FRF to show some motion at higher frequencies. However, the measured data show that the (0,0) mode is excited more significantly in these higher frequency bands. Similarly, the response of the (0,1) mode can be seen to differ significantly from the linear FRF prediction, showing that the system is exhibiting significant nonlinearity, and that any nonlinear model for this system should be one which significantly affects the response in the aforementioned frequency bands.

As described in Section 2.1, it was assumed that the nonlinearities in the system could be adequately modeled by quadratic and cubic functions of the modal displacements. In an initial effort, only the measurements in the frequency range that was excited (i.e. 225 to 245 Hz) were used in the identification. However, this produced a model that was inaccurate at the harmonics of the forcing and so four frequency bands of interest were identified in the figures above, specifically those which showed significant response in Figures 9 and 10 and these were used to define the input data for RFS. The measurements from these four frequency bands were used to populate Eq. (10), and the least squares equation was solved for the nonlinear stiffness terms. Considering nonlinearity in all 13 modes, with coefficients up to cubic and considering all possible nonlinear coupling terms, there were over

600 terms to identify. Initially, numerical ill-conditioning was a challenge, yet after scaling each signal by its RMS value, it was possible to obtain a reliable fit to the measurements.

To evaluate the accuracy of the model found through nonlinear system identification, the restoring force of the system was constructed using the identified parameters, along with the measured displacement, velocity, etc…, The sum of these measured terms multiplied by their respective polynomial terms reproduces the left hand side in Eq. (10), and this was compared with the measured right hand side to see how well the identified parameters reconstruct the response. Figure 11 contains plots of the restoring force reconstructed for the (0,0) mode compared to the measured restoring force. It also contains the same reconstruction obtained using only the linear terms, which were identified from the linear FRFs and are identical to those used to reconstruct the FRFs used to compute the linear response in Figs. 9 and 10. It is interesting to note that the linear RFS prediction matches the measurements quite well, even though the true linear response to the measured forcing in Figs. 9 and 10 showed significant error. This stems from the fact that only the forcing is available as an input when using the FRFs to compute the response (i.e. in Figs. 9 and 10), whereas the RFS method uses the measured acceleration, velocity and displacement as well and these implicitly contain the effect of the nonlinearity. This seems to be a deficiency of the RFS method and deserves further investigation.

Setting that issue aside, one can use the responses in Fig. 11 to evaluate the accuracy of the identified nonlinear model. In order to more easily do this, the error between the measured restoring force and that reproduced by the nonlinear model was computed and is shown in Figure 12. In this figure one can see that the nonlinear model reduces the error near significantly near the first two frequency bands, while leaving it roughly the same at the two higher frequency bands. The same plots for the (0,1) mode can be seen in Figures 13 and 14.

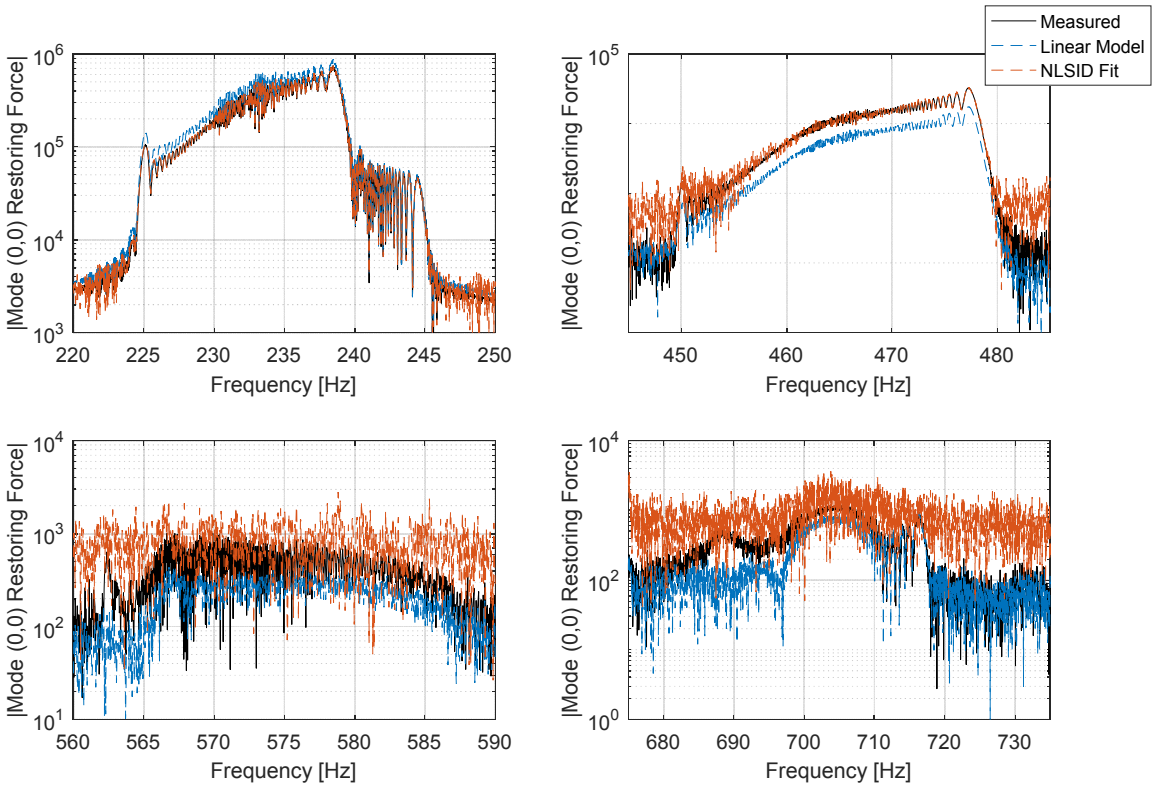

Figure 11: Comparison of the mode (0,0) reconstructed restoring force to the measured restoring force

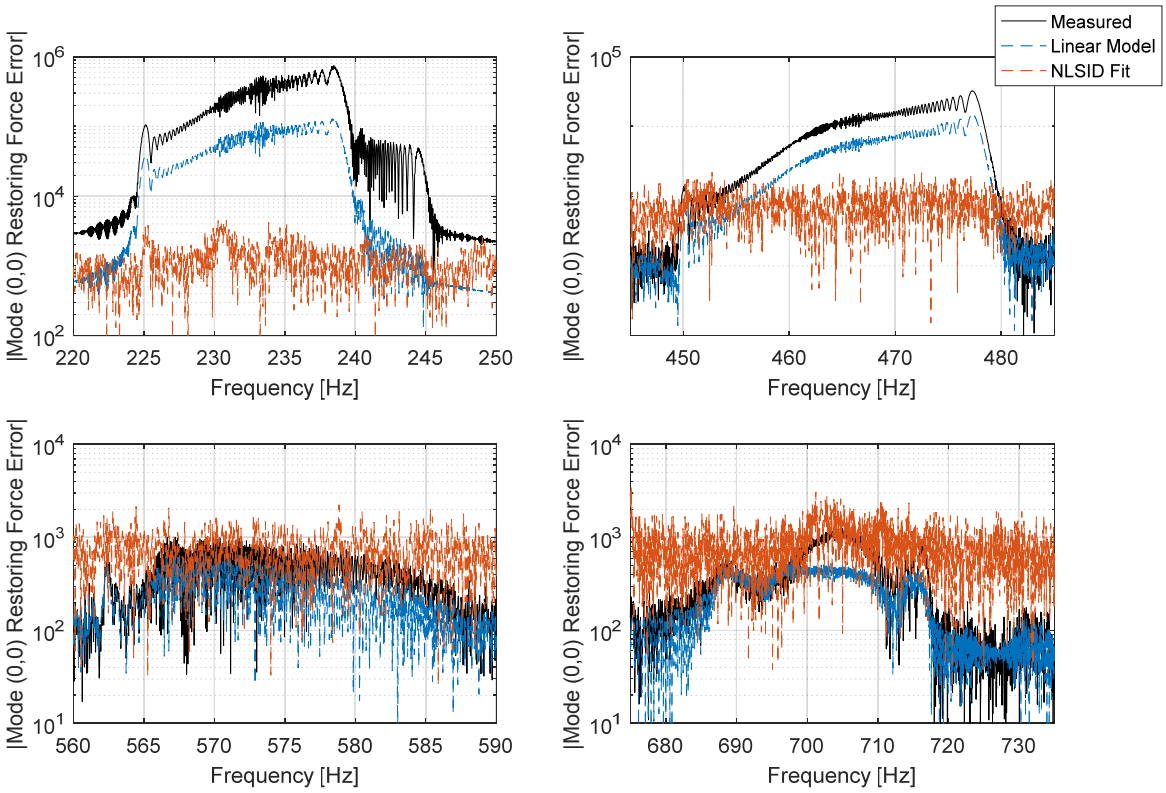

Figure 12: Error in the mode (0,0) reconstructed restoring force compared to the measured restoring force

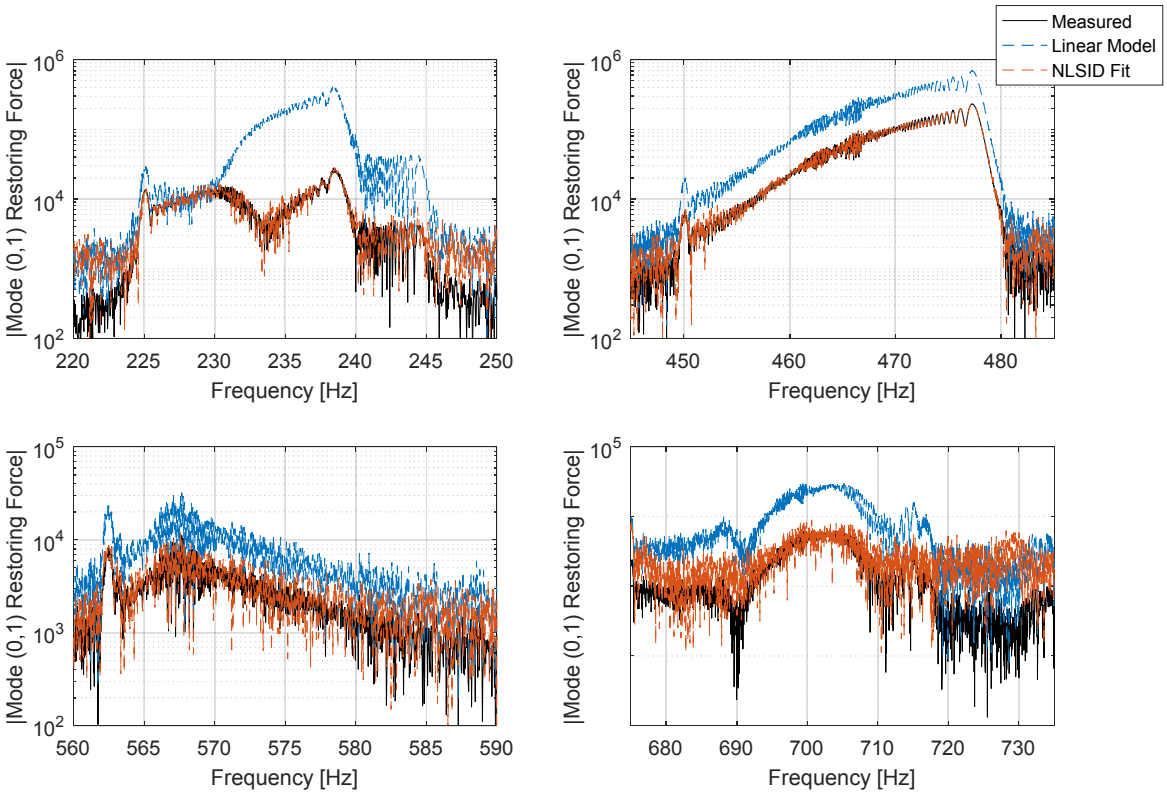

Figure 13: Comparison of the mode (0,1) reconstructed restoring force to the measured restoring force

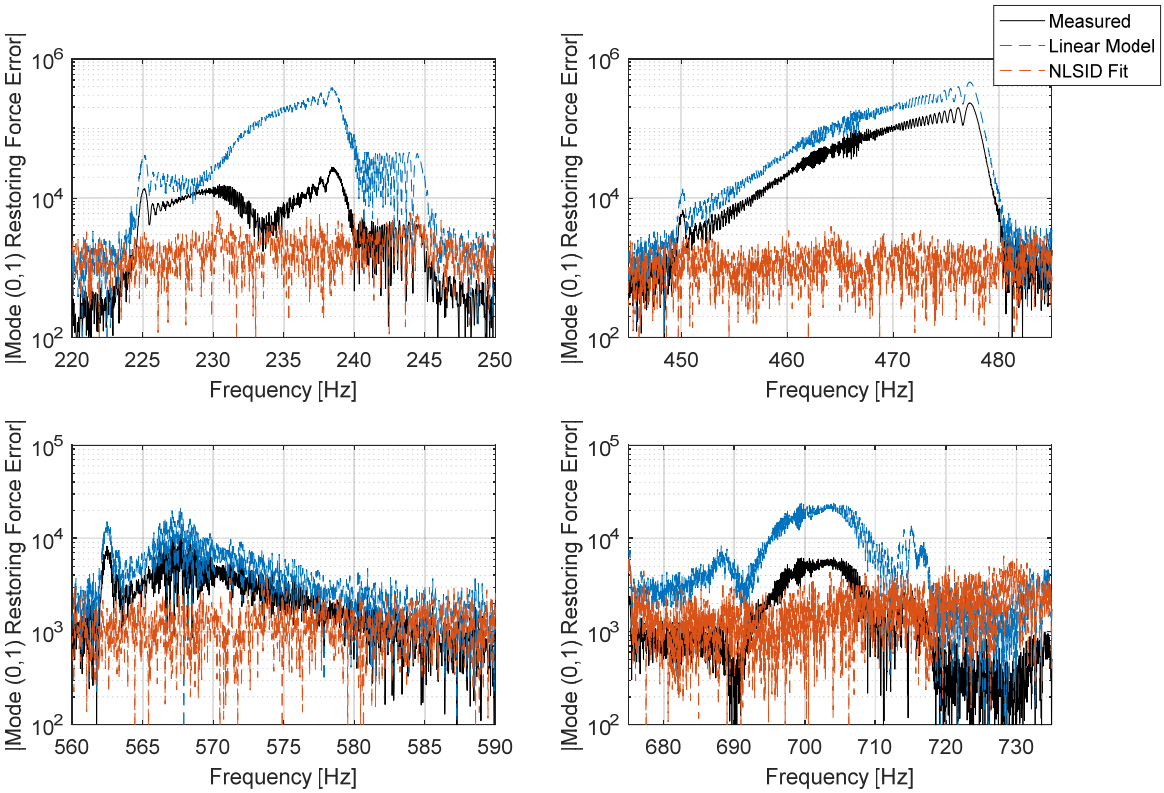

Figure 14: Error in the mode (0,1) reconstructed restoring force compared to the measured restoring force

It can be gathered from the figures above that the nonlinear model is capable of fitting the restoring force of the two modes of interest to a reasonable degree of accuracy across the entire frequency range. Specifically, when compared to a purely linear model, the error in the (0,0) mode restoring force can be seen to decrease by as much as roughly two orders of magnitude near the excited frequency band, and one order of magnitude near the 2nd harmonic of the excited frequency band. In the 3rd and 4th frequency bands, however, no noticeable improvement in error can be seen. The error in the restoring force for the (0,1) mode decreases by similar amounts. Based on this comparison, the identified nonlinear model was considered to be an accurate fit to the dynamics of the system.

The linear and nonlinear stiffness terms for the system were then used in a continuation method, as described in section 2, to solve for the NNMs of the two modes of interest. The NNMs of the nonlinear model were compared to the NNMs of the system measured with the force appropriation method from section 3.2, and this comparison can be seen in Figures 15 and 16. As with Figures 7 and 8, the NNM frequencies were plotted against the RMS of the center point velocity.

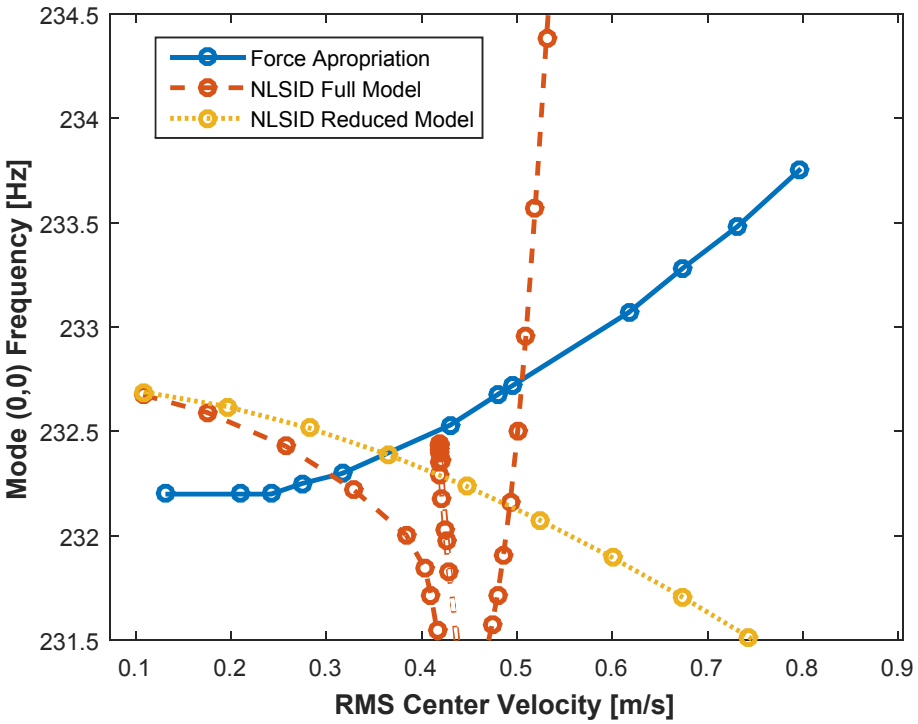

Figure 15: NNM of the (0,0) mode based on Identified (NLSID) model, compared to the NNM measured using force appropriation

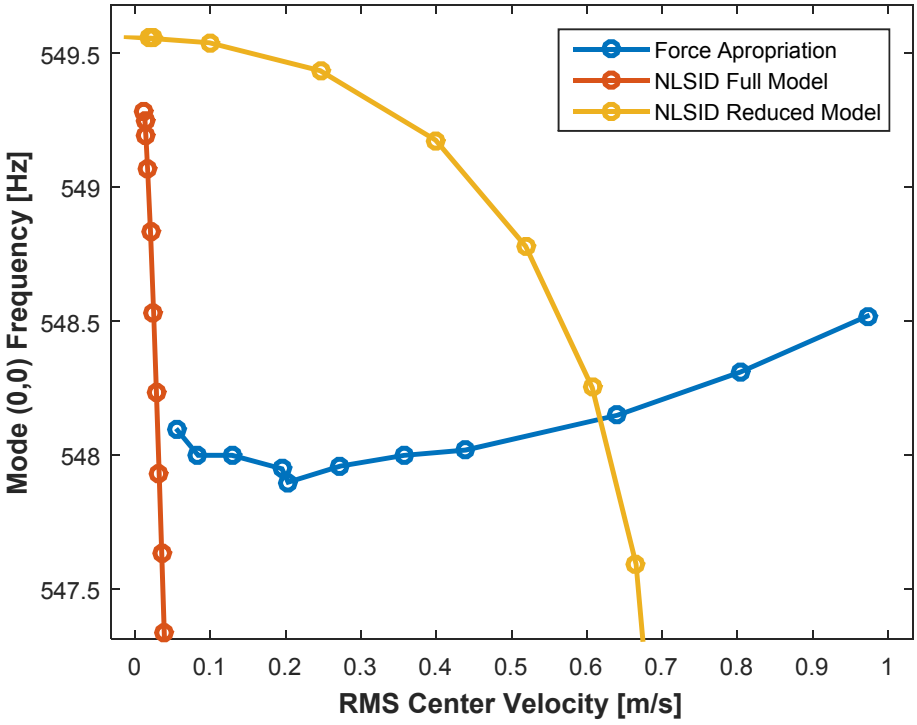

Figure 16: NNM of the (0,1) mode based on Identified (NLSID) model, compared to the NNM measured using force appropriation

It can be seen in Figures 15 and 16 that the identified model is not capable of predicting the NNMs of either mode of interest. Both predicted NNMs can be seen to experience nonlinear behavior at a lower excitation level than the corresponding NNMs measured via force appropriation. Additionally, the nonlinear behavior predicted for each mode differs greatly from the measured phenomena. However, what is even more problematic is that it was discovered that these NNMs were far from unique. In other words, a slight change to the procedure used to identify the modes would change both the quality of the curve fit and the NNMs significantly. To illustrate this, the identification was repeated including the nonlinear terms for only modes 3 and 13, but accounting for linear stiffness and damping of modes 1 through 17 when performing the fit. This was thought to be reasonable since modes 3 and 13 dominate the response, however the resulting model was visibly inferior to the model presented above in terms of the residual error in the least squares problem. In any event, the NNMs of this model were computed, and were found to be dramatically different from those presented earlier, as shown in Figs. 15 and 16.

4. Conclusions

This paper explored the use of system identification in order to determine a nonlinear model which can be used to estimate the NNMs of a system, through the use of a case study on a circular gong. To this end, a low amplitude, random input force was first applied to the system, and the linear modes of the system were found and used to convert the response of the nonlinear (i.e. excited at high amplitude) system to modal coordinates. Then those histories were used to fit a model consisting of nonlinearities that are polynomial functions of the modal displacements. The resulting model satisfied the governing equations of the RFS method quite well at the frequencies where the response was significant, but only after including all of the identified linear modes in the model with every possible cross term. It was surprisingly challenging to obtain a model that produced a low residual error in Eq. (10); models with only a few modes showed significantly larger errors.

Once the best possible system identification model had been obtained, a numerical continuation algorithm was then used to approximate the NNMs of the two modes of interest of the system based on the identified nonlinear stiffness terms. To evaluate the accuracy of the NNMs of the identified model, the force appropriation method was used as in [13] to directly measure the NNM of each mode of interest. It was found that the NNMs predicted by the identified nonlinear model differed greatly from the measured NNMs of the system. The NNMs obtained by system identification varied greatly as the system identification procedure was varied, and so the authors had little confidence in those estimates. In contrast, while the force appropriation method is somewhat slow, as the system was driven with increasing amplitude near each resonance one could tell with high confidence that the NNM had been well approximated based on the phase of the laser velocity and the response. It seemed that even very small frequency shifts of less than 1%, could be measured confidently. Hence, the preliminary conclusion of this work is that force appropriation is preferable to nonlinear system identification when seeking to characterize a geometrically nonlinear system such as this gong. It seems that further research is needed to improve the RFS method before it can be used to confidently compute the response of a system such as this.

Acknowledgements

This work was supported by the Air Force Office of Scientific Research, Award # FA9550-17-1-0009, under the Multi-Scale Structural Mechanics and Prognosis program managed by Dr. Jaimie Tiley. The authors also wish to thank Mike Spottswood other collaborators in the Structural Sciences Center at the Air Force Research Laboratory for their support and for many helpful discussions.

References

[1] M. P. Mignolet, A. Przekop, S. A. Rizzi, and S. M. Spottswood, A review of indirect/non-intrusive reduced order modeling of nonlinear geometric structures. Journal of Sound and Vibration 332 (2013) 2437-2460.

[2] D. A. Ehrhardt, M. S. Allen, T. Beberniss, and S. A. Neild, Finite Element Model Calibration of a Nonlinear Perforated Plate. Journal of Sound and Vibration 392 (2017) 280-294.

[3] R. W. Gordon and J. J. Hollkamp, Reduced-order Models for Acoustic Response Prediction, Air Force Research Laboratory, AFRL-RB-WP-TR-2011-3040, Dayton, OH 2011.

[4] J. J. Hollkamp and R. W. Gordon, Reduced-order models for nonlinear response prediction: Implicit condensation and expansion. Journal of Sound and Vibration 318 (2008) 1139-1153.

[5] J. J. Hollkamp, R. W. Gordon, and S. M. Spottswood, Nonlinear modal models for sonic fatigue response prediction: a comparison of methods. Journal of Sound and Vibration 284 (2005) 1145-63.

[6] R. J. Kuether, B. Deaner, M. S. Allen, and J. J. Hollkamp, Evaluation of Geometrically Nonlinear Reduced Order Models with Nonlinear Normal Modes AIAA Journal 53 (2015) 3273-3285.
[7] D. A. Ehrhardt, R. J. Kuether, and M. S. Allen, Nonlinear Normal Modes in Finite Element Model Validation of Geometrically Nonlinear Flat and Curved Beams, Scitech 2015, 56th AIAA Structures, Structural Dynamics and Materials Confernece, Kissimmee, Florida, 2015.
[8] R. M. Rosenberg, Normal modes of nonlinear dual-mode systems. Journal of Applied Mechanics 27 (1960) 263–268.
[9] G. Kerschen, M. Peeters, J. C. Golinval, and A. F. Vakakis, Nonlinear normal modes. Part I. A useful framework for the structural dynamicist. Mechanical Systems and Signal Processing 23 (2009) 170-94.
[10] A. F. Vakakis, Non-linear normal modes (NNMs) and their applications in vibration theory: an overview. Mechanical Systems and Signal Processing 11 (1997) 3-22.
[11] M. Peeters, G. Kerschen, and J. C. Golinval, Dynamic testing of nonlinear vibrating structures using nonlinear normal modes. Journal of Sound and Vibration 330 (2011) 486-509.
[12] M. Peeters, G. Kerschen, and J. C. Golinval, Modal testing of nonlinear vibrating structures based on nonlinear normal modes: Experimental demonstration. Mechanical Systems and Signal Processing 25 (2011) 1227-1247.
[13] D. A. Ehrhardt and M. S. Allen, Measurement of Nonlinear Normal Modes using Multi-Harmonic Stepped Force Appropriation and Free Decay. Mechanical Systems and Signal Processing (2016)
[14] J.-P. Noël, L. Renson, C. Grappasonni, and G. Kerschen, Identification of nonlinear normal modes of engineering structures under broadband forcing. Mechanical Systems and Signal Processing 74 (2016) 95-110.
[15] S. M. Spottswood and R. J. Allemang, Identification of nonlinear parameters for reduced order models. Journal of Sound and Vibration 295 (2006) 226-45.
[16] S. M. Spottswood and R. J. Allemang, On the investigation of some parameter identification and experimental modal filtering issues for nonlinear reduced order models. Experimental Mechanics 47 (2007) 511-521.
[17] G. Kerschen, K. Worden, A. F. Vakakis, and J.-C. Golinval, Past, present and future of nonlinear system identification in structural dynamics. Mechanical Systems and Signal Processing 20 (2006) 505-592.
[18] M. Ducceschi and C. Touze, Modal approach for nonlinear vibrations of damped impacted plates: Application to sound synthesis of gongs and cymbals. Journal of Sound and Vibration 344 (2015) 313-331.
[19] A. Chaigne, C. Touze, and O. Thomas, Nonlinear vibrations and chaos in gongs and cymbals. Acoustical Science and Technology 26 (2005) 403-409.
[20] G. M. Spelman and R. S. Langley, Statistical energy analysis of nonlinear vibrating systems, ISMA, Leuven, Belgium, 2014.
[21] R. J. Kuether and M. S. Allen, A Numerical Approach to Directly Compute Nonlinear Normal Modes of Geometrically Nonlinear Finite Element Models. Mechanical Systems and Signal Processing 46 (2014) 1–15.
[22] M. Peeters, R. Viguie, G. Serandour, G. Kerschen, and J. C. Golinval, Nonlinear normal modes, part II: toward a practical computation using numerical continuation techniques. Mechanical Systems and Signal Processing 23 (2009) 195-216.
[23] T. Detroux, L. Renson, L. Masset, and G. Kerschen, The harmonic balance method for bifurcation analysis of large-scale nonlinear mechanical systems. Computer Methods in Applied Mechanics and Engineering 296 (2015) 18-38.
[24] R. J. Kuether, L. Renson, T. Detroux, C. Grappasonni, G. Kerschen, and M. S. Allen, Nonlinear Normal Modes, Modal Interactions and Isolated Resonance Curves. Journal of Sound and Vibration 351 (2015)
[25] T. L. Hill, A. Cammarano, S. A. Neild, and D. J. Wagg, Interpreting the forced responses of a two-degree-of-freedom nonlinear oscillator using backbone curves. Journal of Sound and Vibration 349 (2015) 276-288.
[26] R. L. Mayes, B. R. Pacini, and D. R. Roettgen, A Modal Model to Simulate Typical Structural Dynamic Nonlinearity, 34th International Modal Analysis Conference (IMAC XXXIV), Orlando, Florida, 2016.
[27] J. S. Bendat and A. G. Piersol, Engineering Applications of Correlation and Spectral Analysis, Wiley New York, 1980.
[28] M. S. Allen and J. H. Ginsberg, A Global, Single-Input-Multi-Output (SIMO) Implementation of The Algorithm of Mode Isolation and Applications to Analytical and Experimental Data. Mechanical Systems and Signal Processing 20 (2006) 1090–1111.
[29] M. Rades and D. J. Ewins, MIFs and MACs in Modal Analysis, 20th International Modal Analysis Conference (IMAC-20), Los Angeles, CA, 2002.